Dinuclear ruthenium(II) bipyridine complexes having non-symmetric α,α′-diimine based neutral bridging ligands. Synthesis, spectroscopic and electrochemical properties

Soma Chakraborty, Pradip Munshi, Goutam Kumar Lahiri*

Department of Chemistry, Indian Institute of Technology, Bombay, Mumbai-400076, India

Abstract

A group of three dinuclear ruthenium(II) complexes of the type $[(bpy)_2Ru^{II}(L)Ru^{II}(bpy)_2](ClO_4)_4 \cdot 2H_2O$, **1a–1c** [bpy=2,2′-bipyridine, L=bridging ligand, $N_pC_5H_4CH{=}N_i{-}(R){-}N_i{=}CHC_5H_4N_p$; R=none, **1a**; R=$-C_6H_4-$, **1b**; R=$-CH_2-C_6H_4-CH_2-$, **1c**] have been synthesized and characterized. The complexes are essentially diamagnetic and behave as 1:4 electrolytes in acetonitrile solution. The mass of the molecular ion for the complex **1a** and the geometry of the complexes **1** in solution have been assessed by fast atom bombardment (FAB) mass spectrometry and $^1H/^{13}C$ NMR spectroscopy, respectively. Complexes **1** display three metal-to-ligand charge-transfer (MLCT) transitions in the visible region, where the lowest energy MLCT transition is considered to be a $d\pi(Ru^{II})\rightarrow\pi^*$(L) transition. The other two higher energy MLCT transitions are believed to be $d\pi(Ru^{II})\rightarrow\pi^*$(bpy) transitions. Highly intense ligand-based $\pi\rightarrow\pi^*$ transitions are observed in the UV region. In acetonitrile solvent, complexes **1** show one quasi-reversible two-electron oxidation process near 1.5 V vs. Ag/AgCl, due to simultaneous one-electron oxidations [ruthenium (III)⇌ruthenium(II)] of both of the ruthenium centers in **1** and multiple reductions in the range −0.5−−2.7 V vs. Ag/AgCl, due to successive reductions of the coordinated bridging ligand, L, as well as bipyridine. The chemically and electrochemically generated oxidized trivalent congeners of **1** are unstable at room temperature.

Keywords: Dinuclear ruthenium(II) bipyridine complexes; Bridging ligands

1. Introduction

Since the discovery of the important photo-redox activity of $[Ru^{II}(bpy)_3]^{2+}$ (bpy=2,2′-bipyridine) complexes, there has been continuous research activity in the direction of developing new and effective redox catalysts and photosensitizing devices involving the ruthenium–bipyridine moiety [1–14]. In this context, a variety of ruthenium–bipyridine complexes have been prepared and studied over the last 15 years to modulate the ground and excited states' electron transfer and energy transfer processes. The basic strategies behind all of these activities are either to introduce different groups within the bipyridine moiety of $Ru(bpy)_3$ or to substitute one or two bipyridine molecule(s) from the $Ru(bpy)_3$ core by other types of donor sites or by the use of suitable bridging ligands to bring together different ruthenium–bipyridine fragments in the polynuclear array. Although mononuclear systems are extensively studied, current interest is now primarily focused on the supramolecular assemblies of molecular components having well-defined structures and properties [15–28]. Photo-induced energy and electron transfer processes in supramolecular systems can be exploited to develop sensors, light-harvesting and charge separation devices [29,30]. The activity pattern of polynuclear species essentially depend on the nature of the bridging group, which can facilitate the flow of electrons and energy through the molecular components.

The present work originates from our interest in developing a new class of polynuclear ruthenium–bipyridine complexes having neutral α,α′-diimine-based bridging ligands and to study the effect of the nature of the spacers of the bridging center on the electron and charge transfer processes. As a part of our programme, a group of three binuclear ruthenium–bipyridine complexes of the type $[(bpy)_2Ru^{II}N_p,\ N_i{-}(R){-}N_p,\ N_iRu^{II}(bpy)_2]^{4+}$ (R=none,

$-C_6H_4-$, $-CH_2-Ph-CH_2-$) were prepared and their spectroscopic and electrochemical properties have been reported.

To the best of our knowledge, this work demonstrates the first example of polynuclear ruthenium bipyridine complexes incorporating neutral pyridinealdimine-based bridging ligands (L).

2. Experimental

2.1. Materials

Commercially available ruthenium trichloride (S.D. Fine Chemicals, Bombay, India) was converted to $RuCl_3 \cdot 3H_2O$ by repeated evaporation to dryness with concentrated hydrochloric acid. The complex *cis*-$[Ru(bpy)_2Cl_2]\cdot 2H_2O$ was prepared according to the reported procedure [31]. Pyridine-2-aldehyde and α,α′- diamino–*p*-xylene were obtained from Fluka, Switzerland. Other chemicals and solvents were of reagent grade and used as received. For electrochemical studies, HPLC-grade acetonitrile was used. Commercial tetraethyl ammonium bromide was converted to pure tetraethyl ammonium perchlorate (TEAP) by following an available procedure [32].

2.2. Physical measurements

The electrical conductivity of the solution was checked using a Systronic conductivity bridge, 305. Electronic spectra (900–200 nm) were recorded using a Shimadzu UV 2160 spectrophotometer. Infrared spectra were taken on a Nicolet spectrophotometer with samples prepared as KBr pellets. Magnetic susceptibility was checked with a PAR vibrating sample magnetometer. ^1H and ^{13}C NMR spectra were obtained using a 300 MHz Varian FT–NMR spectrometer. Cyclic voltammetry and coulometric measurements were carried out using a PAR model 273A electrochemistry system. A glassy carbon working electrode, a platinum wire auxiliary electrode and a Ag/AgCl reference electrode were used in a three-electrode configuration. TEAP was the supporting electrolyte and the concentration of the solution was $\sim 10^{-3}$ M. The half-wave potential E^0_{298} was set equal to 0.5 ($E_{pa}+E_{pc}$), where E_{pa} and E_{pc} are anodic and cathodic cyclic voltammetric peak potentials, respectively. The scan rate used was 50 mV s^{-1}. A platinum wire gauze working electrode was used in coulometric experiments. All electrochemical experiments were carried out under a dinitrogen atmosphere and are uncorrected for junction potentials. Elemental analyses were carried out using a Perkin-Elmer 240C elemental analyzer. The FAB mass spectrum was recorded on a JEOL SX 102/DA-6000 mass spectrometer.

2.3. Preparation of ligands (L^1–L^3) and complexes (**1a**–**1c**)

The ligands L^1–L^3 were prepared by condensing pyridine-2-aldehyde with the appropriate diamine in a 2:1 mole ratio in dry ethanol following the available procedure [33]. The complexes **1** were synthesized by a general method, and yields varied in the range 55–60%. Details are given for one representative complex **1a** .

2.3.1. $[(bpy)_2Ru^{II}(L^1)Ru^{II}(bpy)_2](ClO_4)_4\cdot 2H_2O$, **1a**

The starting complex $[Ru(bpy)_2Cl_2].2H_2O$ (300 mg, 0.57 mmol) and $AgClO_4$ (240 mg, 1.17 mmol) were placed in dry ethanol (25 cm^3) and the mixture was heated to reflux under stirring conditions for 1 h. The initial violet solution changed to orange–red. It was then cooled and filtered through a Gooch (G-4) sintered-glass funnel. The ligand L^1 (60 mg, 0.29 mmol) was then added to the above filtrate (ethanolato species). The resulting mixture was heated to reflux overnight and it was then cooled. The precipitate thus formed was filtered and washed thoroughly with cold ethanol and benzene. Finally, the product was recrystallized from an acetonitrile–benzene (1:3, v/v) mixture. The yield was 55%.

CAUTION! Perchlorate salts of metal complexes are generally explosive. Care should be taken while handling such complexes.

3. Results and discussion

3.1. Synthesis

The three α,α′-diimine bridging ligands used for the present study are abbreviated as L^1–L^3. The ligands L^1–L^3 differ with respect to the nature of the spacers (R) used in the ligand framework (R=none, $-C_6H_4-$ and $-CH_2-Ph-CH_2$ for L^1–L^3, respectively). The bridging ligands L^1–L^3 bind to the metal ions in a neutral and bidentate N_p,N_i and N_p,N_i (M_2L) manner, forming five-membered chelate rings. The complexes $[(bpy)_2Ru^{II}$ (L) $Ru^{II}(bpy)_2]^{4+}$ **1** have been synthesized from $[Ru^{II}(bpy)_2Cl_2]\cdot 2H_2O$ following the synthetic route shown in Scheme 1. The red-colored cationic complexes **1** were precipitated directly from the respective reaction mixture as dihydrated perchlorate salts, $[(bpy)_2Ru^{II}(L)Ru^{II}(bpy)_2](ClO_4)_4\cdot 2H_2O$. The pure complexes **1** were obtained by recrystallization from a benzene–acetonitrile (1:3, v/v) mixture.

The reactions of the active ruthenium starting complex $[Ru^{II}(bpy)_2(EtOH)_2]^{2+}$ with the ligands, L, always ended up as dimeric complexes **1**, irrespective of the metal–ligand ratio used. The yield of the products varies depending on the metal–ligand ratio and it was found to be

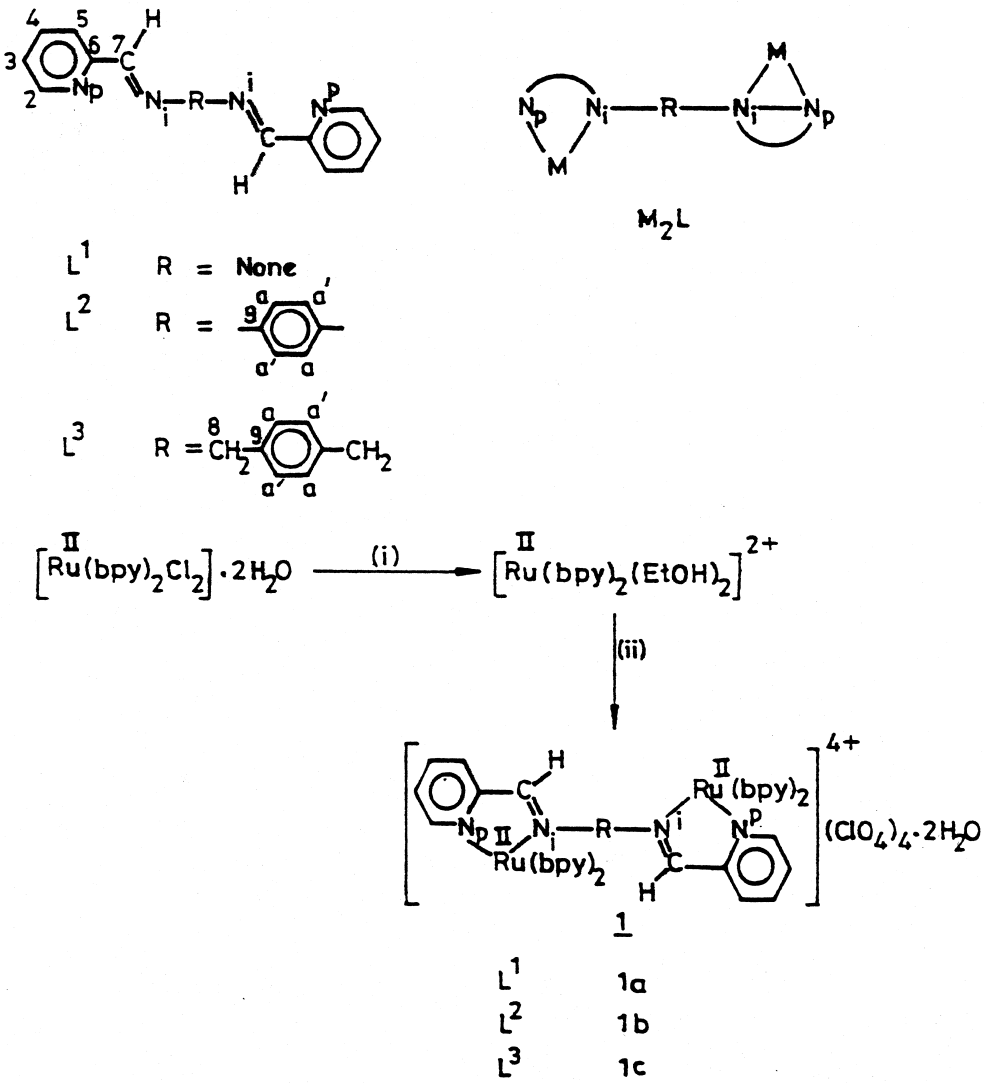

Scheme 1. (i) $AgClO_4$, EtOH, heat, stirring and (ii) L, heat, stirring.

maximum (~60%) in the case of a 2:1 metal–L ratio, as expected. All of our attempts to synthesize the corresponding mononuclear species, $[Ru^{II}(bpy)L]^{2+}$, using lower metal–ligand ratios, of 1:1 or less, have failed completely.

The complexes **1** are highly soluble in polar solvents such as acetonitrile, dimethyl formamide (dmf) and dimethyl sulfoxide (dmso), and are slightly soluble in water, benzene, dichloromethane and chloroform. The extent of solubility varies depending on the nature of the R group present in the ligands L^1–L^3. The microanalytical data (C, H, N) of the complexes are shown in Table 1. The results are in good agreement with the calculated values, which confirm the gross composition of the complexes $[(bpy)_2Ru^{II}(L)Ru^{II}(bpy)_2](ClO_4)_4\cdot 2H_2O$ **1**. The complexes are 1:4 electrolyte in acetonitrile solution (Table 1). Solid state magnetic moment measurements at room temperature (298 K) indicate that all three of the complexes **1a**–**1c** are essentially diamagnetic (low spin Ru^{II}, t_{2g}^6, $S=0$).

The selected IR frequencies of complexes **1** are listed in Table 1. The $\nu_{(C=N)}$ stretching frequency of the free ligands (~1640 cm^{-1}) has been shifted to ~1610 cm^{-1} in accordance with the coordination of the azomethine (CH=N) functions to the metal ions [34]. The strong bands near 1100 and 630 cm^{-1} are observed for all of the complexes due to ionic perchlorate. The ν_{O-H} of the water of crystallization appears near 3400 cm^{-1} as a broad peak. The other expected vibrations of the bipyridine and bridging ligands are systematically present for all of the complexes.

The FAB mass spectrum of one representative complex, **1a**, shows the maximum peak at m/z 1036.6, which corresponds to the molecular ion $[(bpy)_2Ru(L^1)Ru(bpy)_2]^{4+}$ (calculated molecular weight, 1037.2).

Table 1
Microanalytical[a], conductivity[b], infrared[c] and electronic spectral data[b]

Compound	Elemental analysis (%)			Λ_M/Ω^{-1} cm^2 mol^{-1}	IR (cm^{-1}) ν(C=N)	$\nu(ClO_4^-)$	UV/Vis λ_{max}(nm) (ε^d, M^{-1} cm^{-1})
	C	H	N				
1a	42.32 (42.45)	3.10 (3.16)	11.56 (11.43)	444	1611	1124 637	523(9520), 416(15 720), 347[e](15 200), 284(108 320), 246(39 800), 197(95 760)
1b	45.17 (45.02)	3.29 (3.26)	10.73 (10.87)	469	1608	1098 631	480[e](20 120), 429(28 360), 344[e](20 760), 286(103 720), 245(55 480), 200(113 200)
1c	45.87 (45.74)	3.40 (3.46)	10.52 (10.67)	440	1610	1098 637	470(24 560), 420[e](16 000), 359[e](16 640), 288(102 640), 243(51 120), 202(110 400)

[a]Calculated values are in parentheses.
[b]In acetonitrile at 298 K.
[c]In KBr disc.
[d]Extinction coefficient.
[e]Shoulder.

The ^{1}H NMR spectra of the ligands L^1–L^3 and one representative complex, **1b**, in $(CD_3)_2SO$ solvent are shown in Fig. 1a–1d. The observed ^{1}H NMR spectra indicate that each half of the ligand is equivalent due to the presence of internal symmetry. In view of the observed NMR pattern, it may be considered that the *trans* configuration of the ligands is predominant in solution or that there is a fast equilibrium between the *cis* and *trans* isomers of L^1–L^3 [35]. Although the presence of two-fold symmetry make each half of the complexes **1** equivalent, the asymmetric nature of L makes all five pyridine groups around each ruthenium center non-equivalent. The aromatic region of the spectra are complicated due to severe overlapping of several signals, which has precluded the specific identification of individual resonances. However, direct comparisons of the intensity of the aromatic region proton signals with that of the clearly observable azomethine protons (–CH=N–) in the downfield region for all three complexes [δ(–CH=N–), 9.44, 9.12 and 9.40 ppm for **1a**, **1b** and **1c**, respectively] reveal the presence of the expected number of protons for all three complexes. The two phenyl ring protons (a, a′) for the bridging ligands L^2 and L^3 in complexes **1b** and **1c** appear as an AB quartet near 6 ppm (Fig. 1d) and the methylene protons (–CH_2) of the bridging ligand L^3 in complex **1c** appear as a doublet at 5.42 ppm. The singlet due to the azomethine (–CH=N) proton in the complexes **1** is found to be considerably deshielded, δ>9 ppm relative to that of the free ligands, δ~8.5 ppm as a consequence of electron donation to the metal center [36,37].

The decoupled ^{13}C NMR spectra of the ligands (L) in $(CD_3)_2SO$ (Fig. 2a–2c) exhibiting distinct six, eight and nine carbon peaks for L^1, L^2 and L^3, respectively, were as expected. The two phenyl ring carbons (a, a′) for the

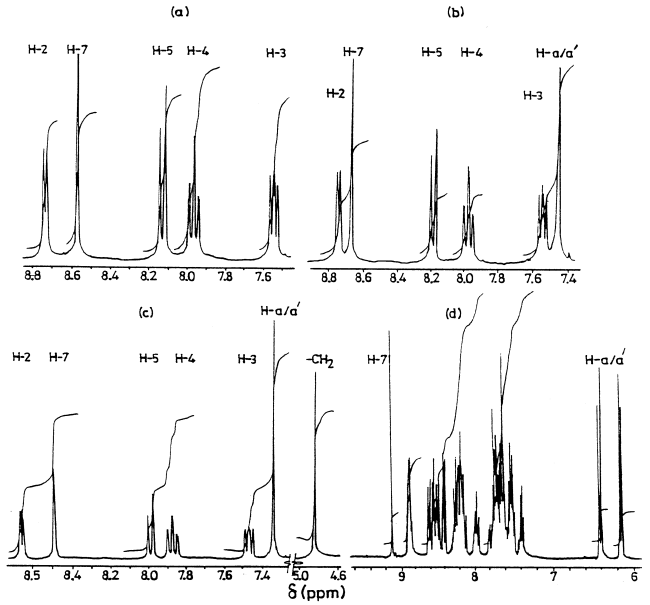

Fig. 1. ^{1}H NMR spectra in $(CD_3)_2SO$ of (a) free L^1, (b) L^2, (c) L^3 and (d) $[(bpy)_2Ru(L^2)Ru(bpy)_2](ClO_4)_4\cdot 2H_2O$, **1b**.

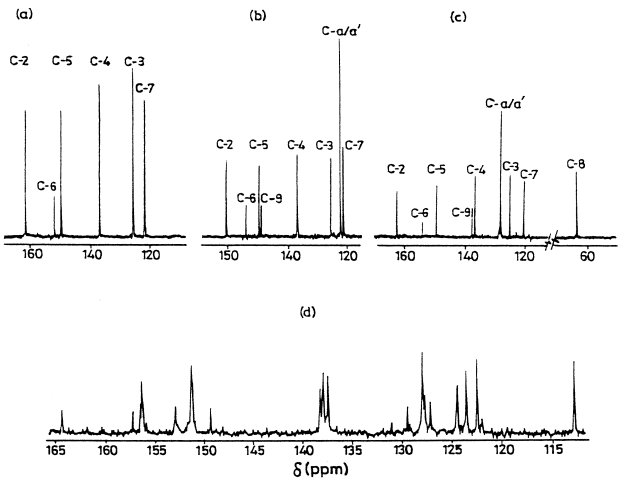

Fig. 2. ^{13}C NMR spectra in $(CD_3)_2SO$ of (a) free L^1, (b) L^2, (c) L^3 and (d) $[(bpy)_2Ru(L^2)Ru(bpy)_2](ClO_4)_4\cdot 2H_2O$, **1b**.

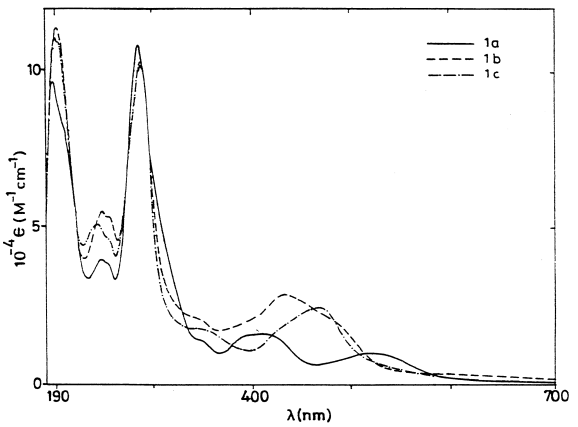

Fig. 3. Electronic spectra of $[(bpy)_2Ru(L^1)Ru(bpy)_2](ClO_4)_4\cdot 2H_2O$, **1a** (———) $[(bpy)_2Ru(L^2)Ru(bpy)_2](ClO_4)_4\cdot 2H_2O$, **1b** (– · –) and $[(bpy)_2Ru(L^3)Ru(bpy)_2](ClO_4)_4\cdot 2H_2O$, **1c** (– · – · –) in acetonitrile at 298 K.

ligands L^2 and L^3 appear together and the $-CH_2$ carbon signal of L^3 appears separately at the upfield region (63.44 ppm).

The ^{13}C NMR spectra of the complexes **1a**, **1b** and **1c** exhibit 26, 29 and 30 signals, respectively. One representative spectrum for complex **1b** is shown in Fig. 2d. Some of the signals appear in a very narrow chemical shift range as overlapping peaks due to their similar electronic environment and that has precluded the identification of the individual signals.

Thus, the FAB mass, ^1H and ^{13}C NMR spectroscopic results along with the microanalytical, conductivity, magnetic moment and IR data collectively establish the composition and stereochemistry of the complexes.

3.2. Electronic spectra

Solution electronic spectra of the complexes **1** were recorded in acetonitrile solvent in the UV/Vis region (200–700 nm). Spectral data are listed in Table 1 and the spectra are shown in Fig. 3. Complex **1a** displays two distinct bands at 523 and 416 nm. The higher energy visible band is associated with a shoulder at 347 nm. Complex **1b** exhibits a band at 429 nm with an associated shoulders at the higher energy part at 480 nm and at the lower energy part at 344 nm. Complex **1c** shows the lowest energy band at 470 nm, which is associated with a shoulder at 420 nm followed by another shoulder at 349 nm. The band positions and profiles are sensitive to the nature of the bridging ligands, L, in the complexes **1**. Although there is a sharp blue shift (40 nm) of the lowest energy band while moving from **1a** to **1b**, only a 10 nm blue shift has been observed on going from **1b** to **1c** (Table 2). Based on the intensity of these visible bands (Table 1), the transitions are assigned to charge transfer in nature [38–40]. The multiple transitions in these complexes may arise due to the presence of different acceptor levels [41]. Since, in these complexes, the ruthenium(II) is in the low-spin t_{2g}^6 state, the observed visible bands are considered to be metal-to-ligand charge-transfer (MLCT) transitions. The lowest energy band is assigned to the $d\pi(Ru^{II})\rightarrow\pi^*L$ transition [42]. This explains the observed shifts in this transition with the change in the bridging ligand in the complexes **1**. This MLCT transition energy decreases in the order of $L=L^3>L^2>L^1$, which suggests that the energy of the lowest unoccupied molecular orbital (LUMO) of the complexes **1** (primarily the π^* orbital energy of α,α'-diimine moieties in the ligands L^1–L^3)

Table 2
Electrochemical data at 298 K[a]

Compound	Ru^{III}–Ru^{II} E^0_{298}/V, (ΔE_p/mV)	Ligand oxidation	Ligand reduction E^0_{298}/V, (ΔE_p/mV)		ΔE^0/V[d]	ν_{MLCT}/cm^{-1}	
						Observed[e]	Calculated[f]
L^1		1.75[b]	−1.50[c],	−1.85[c]			
1a	1.55 (120)		−0.52(90),	−0.96(90),	2.07	19 120	19 694
			−1.62(80),	−1.95(90),			
			−2.45[c],	−2.65[c]			
L^2		1.79[b]	−1.53[c],	−1.87[c]			
1b	1.59 (100)		−0.53(100),	−1.01(110),	2.12	20 833	20 259
			−1.51(80),	−1.85(100),			
			−2.38[c],	−2.57[c]			
L^3		1.80[b]	−1.55[c],	−1.87[c]			
1c	1.56 (90)		−0.59(90),	−1.09(100),	2.15	21 277	20 340
			−1.52(90),	−1.89(100),			
			−2.41[c],	−2.59[c]			

[a]Conditions: Solvent, acetonitrile; supporting electrolyte, NEt_4ClO_4; reference electrode, Ag/AgCl; solute concentration, 10^{-3} M; working electrode, glassy carbon. Cyclic voltammetric data: scan rate, 50 mV s^{-1}; $E^0_{298}=0.5(E_{pc}+E_{pa})$ where E_{pc} and E_{pa} are the cathodic and anodic peak potentials, respectively.
[b]E_{pa} values are considered to be due to the irreversible nature of the voltammograms.
[c]E_{pc} values are considered to be due to the irreversible nature of the voltammograms.
[d]Calculated using Eq. (11).
[e]In CH_3CN solution.
[f]Using Eq. (10).

decreases in the said order. The charge-transfer transition energy is known to depend on the separation in potential between the donor and acceptor levels [43–45]. In the present complexes **1**, the difference in potentials between the first ligand reduction couple (reduction of the bridging ligand L) and the metal oxidation couple (Ru^{II}–Ru^{III}) matches well with the observed lowest energy MLCT transition (see Section 3.4). The other two visible bands near 420 and 350 nm have been assigned on the basis of reported spectra of $[Ru(bpy)_2]^{2+}$ complexes having other kinds of chelating third ligands [46–49]. With respect to the C_2 axis of the bipyridine ligand, there are two different kinds of bipyridine acceptor orbitals, one symmetric (χ) and one antisymmetric (ψ) and the transitions from a metal-filled dπ orbital to these two π^* orbitals results in the above-mentioned bands. The lower energy MLCT band is considered to be due to the dπ(Ru)$\rightarrow\pi^*(\psi)$ and the higher energy MLCT band to the dπ(Ru)$\rightarrow\pi^*(\chi)$ transitions.

The lowest energy MLCT band of $[Ru^{II}(bpy)_3]^{2+}$ appears at 450 nm [50], thus, the replacement of one bpy ligand by an asymmetric ligand L results in a blue-shift of the same transition (429–416 nm). The overall lowering of the molecular symmetry and the increase in charge of the present complexes (+4) with respect to the $Ru(bpy)_3^{2+}$ might be the possible reasons for the observed shift.

In the UV region, the complexes show very intense transitions (Table 1) possibly due to ligand-based π–π^* transitions involving energy levels higher than those of the ligand LUMOs [41].

3.3. Electron-transfer properties

The electron-transfer properties of the complexes have been studied by cyclic voltammetry in acetonitrile solvent (supporting electrolyte, 0.1 M $[NEt_4]ClO_4$; working electrode, glassy carbon). All the potentials are referenced to the Ag/AgCl electrode. The complexes are electroactive with respect to the metal as well as ligand centers and display the same multiple redox processes in the potential range +2–−3 V at 298 K. Voltammograms are shown in Fig. 4, and reduction potentials in Table 2. The assignments of the responses to specific couples are based on the following considerations.

3.3.1. Ruthenium (III)–ruthenium(II) couple

The uncoordinated ligands L display one irreversible oxidation process near 1.75 V (Table 2). The complexes **1** exhibit one quasi-reversible two-electron oxidation process near 1.5 V vs a Ag/AgCl reference electrode (couple I, Fig. 4 and Table 2). Since the oxidative response for the complexes **1** occurs at a less positive potential than that of the free ligands, L, it may therefore be considered that the observed oxidation process for the complexes **1** occurs due to the simultaneous one-electron oxidation of both of the ruthenium centers (Eq. (1)). The two-electron nature of the

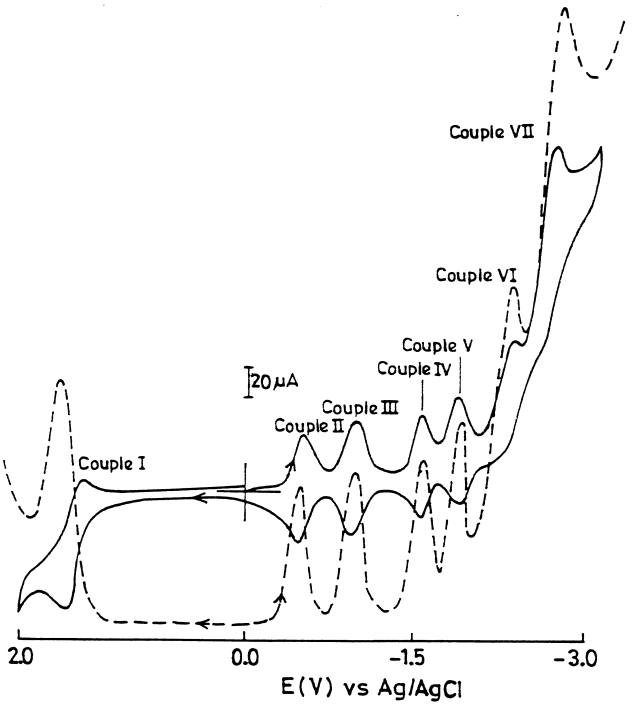

Fig. 4. Cyclic voltammograms and differential pulse voltammograms of a $\sim10^{-3}$ M solution of $[(bpy)_2Ru(L^1)Ru(bpy)_2](ClO_4)_4\cdot2H_2O$, **1a** in acetonitrile at 298 K.

couple I, (Eq. (1)) has been established with the help of differential pulse voltammetric current height and also by constant potential

$$[(bpy)_2Ru^{III}(L)Ru^{III}(bpy)_2]^{6+} + 2e^- \rightleftharpoons [(bpy)_2Ru^{II}(L)Ru^{II}(bpy)_2]^{4+} \quad (1)$$

$[\mathbf{1}]^{2+}$ [**1**]

coulometry ('n' = 2.05, **1a** ; 1.96, **1b**; 2.09, **1c** ; $n = Q/Q'$, where Q' is the calculated Coulomb count for two-electron transfer and Q is that found after exhaustive electrolysis of 10^{-2} mmol of solute. The oxidized trivalent Ru^{III}–Ru^{III} congener is unstable at room temperature.

Under identical experimental conditions, the ruthenium(III)–ruthenium(II) reduction potential of $[Ru(bpy)_3]^{2+}$ appears at 1.29 V [46–50]. Thus, substitution of one bpy ligand from the $[Ru(bpy)_3]^{2+}$ by a α,α'-diimine ligand, L, results in an increase of ruthenium (III)–ruthenium(II) potential by ~0.2 V. The increase in overall charge of the complex cation from +2 in $[Ru(bpy)_3]^{2+}$ to +4 in the complexes **1** provides further electrostatic destabilization of the oxidized species $\mathbf{1}^{2+}$, which possibly has been reflected in the high ruthenium(III)– ruthenium(II) potential of **1**.

3.3.2. Ligand reduction

In acetonitrile solvent, the free ligands L exhibit two irreversible reductions near −1.5 and −1.9 V vs. Ag/

AgCl reference electrode (Table 2). The complexes **1** display six successive quasi-reversible reductions (couples II–VII) in the potential window 0 to −3 V (Fig. 4 and Table 2). Since the first two reductions (couples II and III) occur at much less negative potentials (~ −0.5 and −1.0 V) compared to the first reduction potential of co-ordinated 2,2′-bipyridine ligand of $[Ru(bpy)_3]^{2+}$ (−1.30 V), we therefore believe that the observed first two reductions involve the LUMO of the bridging ligand L. Thus, on coordination, the reversibility of the reduction processes increases and the reduction potentials are ~1.0 V more positive than those of the free ligands L^1–L^3. It may be noted that this is quite consistent with the available data for complexes of ruthenium(II) containing heterocyclic ligands [51–53]. The other observed eight reductions (couples IV–VII) possibly originated from the coordinated bipyridine ligands as expected. 2,2′-Bipyridine is a well known potential electron-transfer center and each bipyridine ligand can accept two electrons in an electrochemically accessible LUMO [54–56]. Since the complexes contain four electroactive ligands, eight successive reductions are therefore expected for each complex in principle. All of the eight expected reductions are actually observed in careful cyclic voltammetric experiments, couples (IV–VII), (Eqs. (2)–(9)).

$$[(bpy)_2Ru^{II}(L)Ru^{II}(bpy)_2]^{2+} + e^- \rightleftharpoons [(b\bar{p}y)(bpy)Ru^{II}(L)Ru^{II}(bpy)_2]^{+} \quad (2)$$

$$[(b\bar{p}y)(bpy)Ru^{II}(L)Ru^{II}(bpy)_2]^{+} + e^- \rightleftharpoons [(b\bar{p}y)(bpy)Ru^{II}(L)Ru^{II}(bpy)(b\bar{p}y)]^{0} \quad (3)$$

$$[(b\bar{p}y)(bpy)Ru^{II}(L)Ru^{II}(bpy)(b\bar{p}y)]^{0} + e^- \rightleftharpoons [(b\bar{p}y)_2Ru^{II}(L)Ru^{II}(bpy)(b\bar{p}y)]^{-} \quad (4)$$

$$[(b\bar{p}y)_2Ru^{II}(L)Ru^{II}(bpy)(b\bar{p}y)]^{-} + e^- \rightleftharpoons [(b\bar{p}y)_2Ru^{II}(L)Ru^{II}(b\bar{p}y)_2]^{2-} \quad (5)$$

$$[(b\bar{p}y)_2Ru^{II}(L)Ru^{II}(b\bar{p}y)_2]^{2-} + e^- \rightleftharpoons [(b\bar{p}y)(b\bar{p}y)Ru^{II}(L)Ru^{II}(b\dot{p}y)_2]^{3-} \quad (6)$$

$$[(b\bar{p}y)(b\bar{p}y)Ru^{II}(L)Ru^{II}(b\dot{p}y)_2]^{3-} + e^- \rightleftharpoons [(b\bar{p}y)(b\bar{p}y)Ru^{II}(L)Ru^{II}(b\dot{p}y)(bpy)]^{4-} \quad (7)$$

$$[(b\bar{p}y)(b\bar{p}y)Ru^{II}(L)Ru^{II}(b\dot{p}y)(bpy)]^{4-} + e^- \rightleftharpoons [(b\bar{p}y)_2Ru^{II}(L)Ru^{II}(b\bar{p}y)(bpy)]^{5-} \quad (8)$$

$$[(b\bar{p}y)_2Ru^{II}(L)Ru^{II}(b\bar{p}y)(bpy)]^{5-} + e^- \rightleftharpoons [(b\bar{p}y)_2Ru^{II}(L)Ru^{II}(b\bar{p}y)_2]^{6-} \quad (9)$$

The one-electron nature of the first reduction (couple II in Fig. 4) is confirmed by constant-potential coulometry in acetonitrile solvent ($n = 0.95$, **1a**; 0.97, **1b**; 1.05, **1c**). The reduced solution is unstable. The one-electron nature of the couples III–V and two- and four-electron stoichiometries of couples VI and VII, respectively, are identified by comparison with the previous first ligand reduction (couple II) with the help of cyclic voltammetric current heights as well as differential pulse voltammetry (Fig. 4). Thus, instead of observing all eight ligand-based reductions separately, only the first two (Eqs. (2) and (3)) appear distinctly (couples IV and V); the other six reductions are observed as simultaneous two-electron reduction (Eqs. (4) and (5), couple VI) and simultaneous four-electron reduction (Eqs. (6)–(9), couple VII).

3.4. Spectroelectrochemical correlation

Complexes **1a, 1b** and **1c** exhibit the lowest energy MLCT transitions of the type $t_2(Ru^{II}) \rightarrow$ ligand LUMO (where LUMO is primarily dominated by the ligand L) at 523, 480 and 470 nm, respectively (Table 1). The quasi-reversible ruthenium(III)–ruthenium(II) reduction potentials are 1.57, 1.52 and 1.54 V, and the first ligand reductions are at −0.50, −0.60 and −0.63 V, respectively. The MLCT transition involves excitation of the electron from the filled t_{2g}^6 orbital of ruthenium(II) to the lowest π^* orbital of the ligand L. The energy of this transition can be predicted from the experimentally observed electrochemical data with the help of Eqs. (10) and (11) [57,58]. Here,

$$\gamma_{MLCT} = 8065(\Delta E^0) + 3000 \quad (10)$$

$$\Delta E^0 = E^0_{298}(Ru^{III} - Ru^{II}) - E^0_{298}(L) \quad (11)$$

$E^0_{298}(Ru^{III}–Ru^{II})$ is the formal potential (in V) of the quasi-reversible ruthenium(III)–ruthenium(II) couple, $E^0_{298}(L)$ is that of the first ligand reduction and γ_{MLCT} is the frequency or energy of the lowest energy charge-transfer band, in cm^{-1}. The factor 8065 is used to convert the potential difference ΔE from V into cm^{-1} and the term 3000 cm^{-1} is of empirical origin. The calculated and experimentally observed γ_{MLCT} transitions are listed in Table 2 and there is a linear relationship between the γ_{MLCT} and ΔE (Table 2). Here, the calculated and observed values lie within 1000 cm^{-1} of the experimentally observed γ_{MLCT} energies, and are in good agreement with the earlier observation on other mixed ligand ruthenium–bipyridine complexes [59–61].

4. Conclusions

We have observed the effect of neutral α,α′-diimine-based bridging ligands (L) on the redox and spectroscopic properties of the $[Ru(bpy)_2]$ core. The presence of strong π-acidic pyridinealdimine-based bridging ligand (L) along with the $[Ru(bpy)_2]$ core destabilizes the oxidized trivalent

congener of **1** and this is reflected in the high ruthenium(II)–ruthenium(III) oxidation potential of the complexes **1**. The complexes **1** display multiple ligand reductions due to successive electron-transfer processes on both the bridging ligand (L) and bipyridine molecules. The lowest energy MLCT transition for the complexes involves the LUMO of the bridging ligand whereas the higher energy MLCT transitions involve the orbitals primarily dominated by the bipyridine ligands. The correlation between the energies of the lowest MLCT absorption bands and the electrochemical redox potentials follow an excellent linear relationship, in accordance with the other $Ru(bpy)_2L$ complexes.

Acknowledgements

Financial support received from the Department of Science and Technology, New Delhi, India, is gratefully acknowledged. Special acknowledgement is made to the Regional Sophisticated Instrumentation Center (RSIC), I.I.T., Bombay, for providing the NMR facility. The referees comments at the revision stage were very helpful.

References

[1] J.P. Collin, R. Kayhanian, J.P. Sauvage, G. Calogero, F. Barigelletti, A.D. Cian, J. Fischer, J. Chem. Soc. Chem. Commun. (1997) 775.
[2] B.J. Coe, D.A. Friesen, D.W. Thompson, T.J. Meyer, Inorg. Chem. 35 (1996) 4575.
[3] M.D. Ward, Inorg. Chem. 35 (1996) 1712.
[4] S.C. Rasmussen, D.W. Thompson, V. Sing, J.D. Petersen, Inorg. Chem. 35 (1996) 3449.
[5] K.D. Keerthi, B.K. Santra, G.K. Lahiri, Polyhedron 17 (1998) 1387.
[6] B.K. Santra, M. Menon, C.K. Pal, G.K. Lahiri, J. Chem. Soc., Dalton Trans. (1997) 1387.
[7] A.M.W. Cargill-Thompson, J.C. Jeffery, D.J. Liard, M.D. Ward, J. Chem. Soc., Dalton Trans. (1996) 879.
[8] A. Juris, V. Balzani, F. Barigelletti, S. Campagna, P. Belser, A.V. Zelewsky, Coord. Chem. Rev. 84 (1988) 85.
[9] K. Kalyansundaram, Coord. Chem. Rev. 28 (1989) 2920.
[10] T.J. Meyer, Pure. Appl. Chem. 58 (1986) 1193.
[11] L. Fabbrizzi, A. Poggi, Chem. Soc. Rev. (1995) 197.
[12] M.D. Ward, Chem. Soc. Rev. (1995) 121.
[13] D. Gust, T.A. Moore, A.L. Moore, Acc. Chem. Res. 115 (1993) 5975.
[14] B. O'Regan, M. Gratzel, Nature 353 (1991) 738.
[15] V. Marvaud, D. Astruc, J. Chem. Soc. Chem. Commun. (1997) 773.
[16] C. Kaes, M.W. Hosseini, R. Ruppert, A.D. Cian, J. Fischer, J. Chem. Soc. Chem. Commun. (1995) 1445.
[17] N.A. Lewis, W. Pan, Inorg. Chem. 34 (1995) 2244.
[18] N.C. Fletcher, F.R. Keene, H. Viebrock, A.V. Zelewsky, Inorg. Chem. 36 (1997) 1113.
[19] V.W. Wah Yam, V.W.M. Lee, F. Ke, K.W.M. Siu, Inorg. Chem. 36 (1997) 2124.
[20] J.M. Lehn, Angew. Chem. Int. Ed. Engl. 27 (1988) 89.
[21] S. Lloyd, Science 261 (1993) 1569.
[22] J.J. Hopfield, J.N. Onuchie, D.N. Beratan, J. Phys. Chem. 93 (1989) 6350.
[23] M.R. Wasielewski, Chem. Rev. 92 (1992) 435.
[24] V. Balzani, F. Scandola, Supramolecular photochemistry, Horwood, Chichester, 1991.
[25] J.M. Lehn, Angew. Chem. Int. Ed. Engl. 29 (1990) 1304.
[26] E.C. Constable, Adv. Inorg. Chem. Radiochem. 30 (1986) 69.
[27] F. Scandola, M.T. Indelli, C. Chiorboli, C.A. Bignozzi, Top. Curr. Chem. 158 (1990) 73.
[28] M. Haga, M.M. Ali, H. Maegawa, K. Nozaki, A. Yoshimura, T. Ohno, Coord. Chem. Rev. 99 (1994) 132.
[29] V. Balzani, L. Moggi, F. Scandola, in: V. Balzani (Ed.), Supramolecular photochemistry, Balzani, Reidel, Dordrecht, 1981, p. 1.
[30] V. Balzani, A. Juris, M. Venturi, S. Campagna, S. Serroni, Chem. Rev. 96 (1996) 759.
[31] B.P. Sullivan, D.J. Salmon, T.J. Meyer, Inorg. Chem. 17 (1978) 3334.
[32] D.T. Sawyer, A. Sobkowiak, J.L. Roberts Jr., Electrochemistry for chemists, second ed, Wiley, New York, 1995.
[33] W.J. Stratton, D.H. Busch, J. Am. Chem. Soc. 80 (1958) 1286.
[34] R. Hariram, B.K. Santra, G.K. Lahiri, J. Organomet. Chem. 540 (1997) 155.
[35] M.A. Haga, K. Koizumi, Inorg. Chim. Acta 104 (1985) 47.
[36] T.L. James, Nuclear magnatic resonance in biochemistry. Academic Press, New York, 1975.
[37] B. Pesce, Nuclear magnetic resonance in chemistry. Academic Press, New York, 1965.
[38] B.K. Santra, G.K. Lahiri, J. Chem. Soc., Dalton Trans. (1998) 139.
[39] B.K. Santra, G.K. Lahiri, J. Chem. Soc., Dalton Trans. (1997) 1883.
[40] B.K. Santra, G.K. Lahiri, J. Chem. Soc., Dalton Trans. (1997) 129.
[41] S. Choudhury, A.K. Deb, S. Goswami, J. Chem. Soc., Dalton Trans. (1994) 1305.
[42] V. Balzani, D.A. Bardwell, F. Barigelletti, R.L. Cleary, M. Guardigli, J.C. Jeffery, T. Sovrani, M.D. Ward, J. Chem. Soc., Dalton Trans. (1995) 3601.
[43] M. Haga, E.S. Dodsworth, A.B.P. Lever, Inorg. Chem. 25 (1986) 447.
[44] E.S. Dodsworth, A.B.P. Lever, Chem. Phys. Lett. 119 (1985) 61.
[45] N. Bag, A. Pramanik, G.K. Lahiri, A. Chakravorty, Inorg. Chem. 31 (1992) 40.
[46] A. Ceulemansm, L.G. Vanquickenborne, J. Am. Chem. Soc. 103 (1981) 2238.
[47] M.J. Root, E. Deutsch, Inorg. Chem. 14 (1985) 1464.
[48] R. Alsfasser, R.V. Elidik, Inorg. Chem. 35 (1996) 628.
[49] B.J. Coe, T.J. Meyer, P.C. White, Inorg. Chem. 34 (1995) 593.
[50] G.M. Brown, T.R. Weaver, F.R. Keene, T.J. Meyer, Inorg. Chem. 15 (1976) 190.
[51] S. Goswami, R.N. Mukherjee, A. Chakravorty, Inorg. Chem. 22 (1983) 2825.
[52] N.E. Tokel-Takvoryan, R.W. Hemingway, A.J. Bard, J. Am. Chem. Soc. 95 (1973) 6582.
[53] R.J. Crutehley, A.B.P. Lever, Inorg. Chem. 21 (1982) 2276.
[54] S. Bhattacharya, Polyhedron 12 (1993) 235.
[55] C.M. Elliott, J. Chem. Soc. Chem. Commun. (1980) 261.
[56] D.E. Morris, K.W. Hanck, M.K. DeArmond, Inorg. Chem. 24 (1985) 977.
[57] A.A. Vlcek, E.S. Dodsworth, W.J. Pietro, A.B.P. Lever, Inorg. Chem. 34 (1995) 1906.
[58] B.K. Ghosh, A. Chakravorty, Coord. Chem. Rev. 95 (1989) 239.
[59] B.P. Sullivan, J.V. Caspar, S.R. Johnson, T.J. Meyer, Organometallics 3 (1984) 1241.
[60] E.S. Dodsworth, A.B.P. Lever, Chem. Phys. Lett. 124 (1986) 152.
[61] M.A. Greaney, C.L. Coyle, H.A. Harmer, A. Jordan, E.I. Stiefel, Inorg. Chem. 28 (1989) 912.